A quantitative approach to painting styles

Vilson Vieira *, Renato Fabbri, David Sbrissa, Luciano da Fontoura Costa, Gonzalo Travieso

Instituto de Física de São Carlos, Universidade de São Paulo (IFSC/USP), Brazil

HIGHLIGHTS

- Applied statistical mechanics methods to the analysis of painting styles.
- Philosophical concepts like dialectics were modeled as quantitative metrics.
- Wider dispersion of characteristics for Modern Art while superposition for Baroque.
- Confirms art history: Moderns are independent in style while Baroques share techniques.
- Painting shows increasing innovation. High opposition in Baroque–Modern transition.

ARTICLE INFO

ABSTRACT

This research extends a method previously applied to music and philosophy (Vilson Vieira et al., 2012), representing the evolution of art as a time-series where relations like *dialectics* are measured quantitatively. For that, a corpus of paintings of 12 well-known artists from baroque and modern art is analyzed. A set of 99 features is extracted and the features which most contributed to the classification of painters are selected. The projection space obtained provides the basis to the analysis of measurements. These quantitative measures underlie revealing observations about the evolution of painting styles, specially when compared with other humanity fields already analyzed: while music evolved along a master–apprentice tradition (high dialectics) and philosophy by opposition, painting presents another pattern: constant increasing skewness, low opposition between members of the same movement and opposition peaks in the transition between movements. Differences between baroque and modern movements are also observed in the projected "painting space": while baroque paintings are presented as an overlapped cluster, the modern paintings present minor overlapping and are disposed more widely in the projection than the baroque counterparts. This finding suggests that baroque painters shared aesthetics while modern painters tend to "break rules" and develop their own style.

© 2014 Elsevier B.V. All rights reserved.

1. Introduction

Painting classification is a common field of interest for applications such as painter identification – e.g. assessing the authenticity of a given art work – style classification, paintings database search and more recently, automatic aesthetic judgment in computational creativity applications. Determining the best features for painting style characterization is a complex task on its own. Many studies [1–4] applied image processing to feature extraction for painter and art movements

---

* Corresponding author. Tel.: +55 016981087007.

E-mail addresses: vilson@void.cc (V. Vieira), fabbri@usp.br (R. Fabbri), davidsbrissa@hotmail.com (D. Sbrissa), ldfcosta@gmail.com (L. da Fontoura Costa), gonzalo@ifsc.usp.br (G. Travieso).

identification. Manovich [5–7] uses features like entropy, brightness and saturation to map paintings and general images into a 2-dimensional space and, in this way, to visualize the difference between painters. There are also many related works dealing on feature selection for painting classification. Penousal et al. [8] use features based on aesthetic criteria estimated by image complexity while Zujovic et al. [9] evaluate a large set of features that most contribute to classification.

This study also analyzes a set of features which most contribute to the classification of paintings. Although, in contrast with previous works, it goes forward: the historic evolution of painting styles is analyzed by means of geometric measures in the feature space. Those measures are based on key concepts from Philosophy: *opposition*, *skewness* and *dialectics*. The dialectics, for instance, is defined by Hegel [10] as a method of argument where a synthesis solves the tension between two opposing ideas: thesis and antithesis. Those concepts are originally qualitative. In this study, thesis, antithesis and synthesis are defined as states in a time-series. The dialectics is then calculated as a quantitative measure: it is defined as the inverse distance between the synthesis state and the perpendicular bisector between thesis and antithesis states. The lower the distance, the greater the dialectics, because the synthesis state is near the perpendicular bisector that models the *ideal synthesis*. This quantitative approach is not meant to surpass the qualitative approach but to contribute in the understanding of human history.

To create the feature space, a set of 99 features is extracted from 240 images of 12 well-known painters. The first six painters of this group represent the baroque movement while the remaining six represent the modern art period. A feature selection process yields the pair of features which most contributed for the classification. Similar results using LDA (Linear Discriminant Analysis) are obtained, which reinforce the feature selection method.

After feature selection, a centroid for each group of paintings is calculated which defines a *prototype*: a representative work-piece for the respective cluster. The set of all prototypes following a chronological order defines a time-series where the main purpose of this study is performed: the quantitative analysis of the historical evolution of art movements. Extending a method already applied to music and philosophy, [11] *opposition*, *skewness* and *dialectics* measurements are taken. These concepts are central in philosophy – e.g. philosophers from antiquity like Aristotle and Plato developed their ideas using the dialectics method while it is also found in modern works like Hegelian and Marxist dialectics – and humanistic fields, however lack studies from a quantitative perspective [10]. Represented as geometric measures, these concepts reveal interesting results and patterns. Modern paintings groups show minor superposition when compared with baroque counterparts suggesting the independence in style found historically in modernists and strong influence of shared painting techniques found in baroque painters. Dialectics and opposition values presented a peak in the transition between baroque and modern periods – as expected considering history of art – with decreasing values in the beginning of each period. Skewness index is presented with oscillating but increasing values during all the time-series, suggesting a constant innovation through art movements. These results present an interesting counterpart with previous results in philosophy – where opposition is strong in almost entire time-series – and in music—where the dialectics is remarkable [11].

The study starts describing the corpus of paintings used and a review of both aesthetic and historic facts regarding baroque and modern movements (Section 2). The image processing steps used to extract features from these paintings are presented followed by the feature selection. The results are then discussed in Section 3 with basis on geometric measurements in the projected feature space—considering the most clustered projection and LDA components.

2. Modeling painting movements

2.1. Painting corpus

A group of 12 well-known painters is selected to represent artistic styles or movements from baroque to modernism. Six painters are chosen to represent each of these movements. The group is presented in Table 1 together with their more representative style, in chronological order. It is known that painters like Picasso covered more than one style during his life. For example, only the Cubist style is considered for Picasso, even though the artist developed other styles during his career.

For each painter, 20 raw images are considered from the database of public images organized by Wikipedia. Examples of selected paintings titles and their respective creation years are listed in Table 2 and all the paintings are listed in Table B.1 in Appendix B.[1]

It is interesting to review some historical and aesthetic characteristics from baroque and modern movements before entering into the quantitative analysis in Section 3 where those hypotheses are further discussed. Baroque is marked by tradition, a desire to portray the truth (found in Caravaggio, Frans Hals and Velázquez), the beauty (Poussin, Vermeer), the nature and the sacred (Caravaggio, Rembrandt). A remarkable use of light contrast (as in the "*chiaroscuro*" technique mastered by Caravaggio), disregarding simple equilibrium in composition and preference for complex oppositions, both compound aesthetic characteristics which baroque artists used to represent their ideas. The transmission of those techniques from one painter to another is common in baroque. Modernists, on the other hand, did not follow "rules". Each modern painter employed or created new ways to represent ideas. As noted by Gombrich: "[they] craved for an art that does not consist of tricks that could be learned, for a style that is not a mere style, but something strong and powerful like the human

---

[1] The source code together with all the 240 raw images are available online at http://github.com/automata/ana-pintores.

Table 1
Painters ordered chronologically with the artistic style they represent.

Artists	Remarkable styles/movements
Caravaggio	Baroque, Renaissance
Frans Hals	Baroque, Dutch Golden Age
Nicolas Poussin	Baroque, Classicism
Diego Velázquez	Baroque
Rembrandt	Baroque, Dutch Golden Age, Realism
Johannes Vermeer	Baroque, Dutch Golden Age
Vincent van Gogh	Post-Impressionism
Wassily Kandinsky	Expressionism, Abstract art
Henri Matisse	Modernism, Impressionism
Pablo Picasso	Cubism
Joan Miró	Surrealism, Dada
Jackson Pollock	Abstract expressionism

passion" [12]. van Gogh pursued this artistic trend in his intense use of colors and the caricature aspect of his paintings. Paul Gauguin searched for "primitive" in his paintings. Others, like Seurat, applied physical properties of the chromatic vision and started painting the nature like a collection of color points, and ended creating the pointillism. Modernists created a new style for each of their experiments using their own techniques to represent a nature outside the domains already covered by their predecessors.

2.2. Image processing

All 240 images are resized to 800×800 pixels and cropped to consider a region positioned in the same coordinates and with same aspect for all original paintings. Although details are lost from the original image, windowing is necessary as the paintings have varying sizes and aspect ratios (for instance, Pollock has paintings with larger width than height when compared with Caravaggio or van Gogh) and some of the image measurements are size dependent. After windowing, the images are pre-processed by applying histogram equalization and median filtering with a 3-size window. Feature extraction algorithms are applied to colored, gray-scale or binary versions of images as necessary (e.g. convex-hull used a binary image, whereas Haralick texture used the gray-scale image and SLIC segmentation analysis was applied to color images). Curvature measurements are extracted from segments of paintings identified by the SLIC segmentation method [13] as presented in Fig. 2. The whole process is represented schematically in Fig. 1 and covers all the steps from image processing through measurements, discussed in the following sections.

2.3. Extracted features

To create a *painting space* a number of distinct features extracted by computational methods from raw images of the paintings are considered. The features are related with aesthetic characteristics and aim to quantify properties well-known by art critics. All the features are summarized in Table 3 and detailed, grouped in classes, in the following list.

Shape features: after image segmentation, a number of shape descriptors are calculated for each segment, represented as a binary matrix. *Perimeter* is measured as pixel-length of the segment contour. *Area* is estimated by counting the number of pixels representing the segment. A convex-hull of the segment is used to calculate the *convex area* and its ratio to the original segment area. The *number of constituent segments* for each painting is also considered as a descriptor. *Circularity* reveals how much a shape remembers a circle and is obtained by the ratio between perimeter and area of the segment.

Texture and complexity features: to estimate image complexity, a number of *entropy* measures of its energy (squared FFT coefficients) are computed—listed in the first quarter of Table 3. Together with entropy, a more specific family of measurements is considered for texture characterization: the 14 *Haralick texture features* [14] are calculated for this purpose.

Curvature: this descriptor has an interesting biological motivation related to the human visual system—e.g. object recognition is related to the identification of corners and high curvature points [15]. These points have more information about object shape than straight lines or smooth curves. In this sense, curvature is well suited for the characterization of the considered paintings. Curvature $k(t)$ of a parametric curve $c(t) = (x(t), y(t))$ is defined as:

$$k(t) = \frac{\dot{x}(t)\ddot{y}(t) - \dot{y}(t)\ddot{x}(t)}{(\dot{x}(t)^2 + \dot{y}(t)^2)^{\frac{3}{2}}} \tag{1}$$

t being the arc-length parameter and $\dot{x}(t)$, $\dot{y}(t)$, $\ddot{x}(t)$ and $\ddot{y}(t)$ are respectively the first and second order derivatives of $x(t)$ and $y(t)$. These derivatives are obtained through Fourier transform and convolution theorem:

$$\dot{x} = \Im^{-1}(2\pi i\omega X(\omega)) \tag{2}$$

$$\dot{y} = \Im^{-1}(2\pi i\omega Y(\omega)) \tag{3}$$

Table 2
Some of the 240 selected paintings and their respective authors and year of creation. All the paintings are listed in Appendix B in Table B.1.

Painter	Painting title	Year
Caravaggio	Musicians	1595
	Judith Beheading Holofernes	1598
	David with the Head of Goliath	1610
Frans Hals	Portrait of an unknown woman	1618/20
	Portrait of Paulus van Beresteyn	1620s
	Portrait of Stephanus Geeraerdts	1648/50
Nicolas Poussin	Venus and Adonis	1624
	Cephalus and Aurora	1627
	Acis and Galatea	1629
Diego Velázquez	Three musicians	1617/18
	The Lunch	1618
	La mulatto	1620
Rembrandt	The Spectacles-pedlar (Sight)	1624/25
	The Three Singers (Hearing)	1624/25
	Balaam and the Ass	1626
Johannes Vermeer	The Milkmaid	1658
	The Astronomer	1668
	Girl with a Pearl Earring	1665
Vincent van Gogh	Starry Night Over the Rhone	1888
	The Starry Night	1889
	Self-Portrait with Straw Hat	1887/88
Wassily Kandinsky	On White II	1923
	Composition X	1939
	Points	1920
Henri Matisse	Self-Portrait in a Striped T-shirt	1906
	Portrait of Madame Matisse	1905
	The Dance (first version)	1909
Pablo Picasso	Les Demoiselles d'Avignon	1907
	Guernica	1937
	Dora Maar au Chat	1941
Joan Miró	The Farm	1921/22
	The Tilled Field	1923/24
	Bleu II	1961
Jackson Pollock	No. 5	1948
	Autumn Rhythm	1950
	Blue Poles	1952

$$\ddot{x} = \Im^{-1}(-(2\pi\omega)^2 X(\omega)) \tag{4}$$

$$\ddot{y} = \Im^{-1}(-(2\pi\omega)^2 Y(\omega)) \tag{5}$$

where $\Im^{-1}$ is the inverse Fourier transform, X and Y are the Fourier transform of x and y respectively, ω is the angular frequency and i is the imaginary unit (see Fig. 2).

The calculation of the derivatives $(\dot{x}(t), \dot{y}(t))$ and $(\ddot{x}(t), \ddot{y}(t))$ by a numerical method (i.e. Fourier transform) is sensitive to high frequency noise [15]. A low-pass filter can be used to compensate this effect. A Gaussian filter is then applied to the signal and defined as

$$g(t) = \frac{1}{2\pi\sigma^2} \exp\left(-\frac{t^2}{2\sigma^2}\right) \tag{6}$$

and its Fourier transform is given by

$$G(\omega) = \exp\left(\frac{-(2\pi)^2\omega^2}{(2/\sigma)^2}\right). \tag{7}$$

Using the convolution theorem it is possible to apply the Gaussian filter $g(t)$ to the signal:

$$\hat{\dot{x}}(t) = \dot{x} * g(t) = \Im^{-1}\left(\dot{X}(\omega)G(\omega)\right) \tag{8}$$

$$\hat{\dot{y}}(t) = \dot{y} * g(t) = \Im^{-1}\left(\dot{Y}(\omega)G(\omega)\right) \tag{9}$$

$$\hat{\ddot{x}}(t) = \ddot{x} * g(t) = \Im^{-1}\left(\ddot{X}(\omega)G(\omega)\right) \tag{10}$$
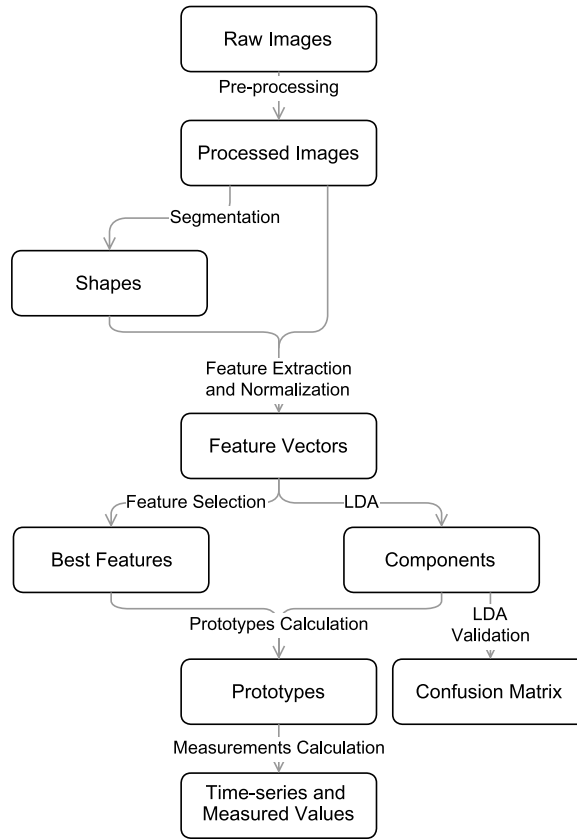
Fig. 1. A summary of all steps from image processing through feature extraction through time-series and measurements calculation (skewness, opposition and dialectics).

$$\hat{\ddot{y}}(t) = \ddot{y} * g(t) = \Im^{-1}\left(\ddot{Y}(\omega)G(\omega)\right) \tag{11}$$

where $*$ represents the convolution operation, obtaining the first and second order multi-scale derivatives $(\hat{\dot{x}}(t), \hat{\dot{y}}(t))$ and $(\hat{\ddot{x}}(t), \hat{\ddot{y}}(t))$ for both $x(t)$ and $y(t)$. These are the derivatives used to calculate curvature $k(t)$ (Eq. (1)) free from high frequency noise.

The corresponding features are calculated from the curvature $k(t)$: the *mean* and *standard deviation* of data, the *number of peaks* and the *distance* (geometric and in pixels) between peaks. It is important to note that a *peak* is defined as a high curvature point. A point a is considered a peak if its curvature $k(a)$ satisfies the following criteria:

$$k(a) > k(a-1) \tag{12}$$
$$k(a) > k(a+1) \tag{13}$$
$$k(a) > \tau \tag{14}$$

τ being the corresponding threshold defined as

$$\text{median}\,(k)\,\gamma \tag{15}$$

where γ is a factor obtained empirically as values which reveal the desired level of curvature details.

2.4. Measurements

N_f features define an N_f-dimensional space, also called *painting space* where the following measurements are calculated [11]. For simplification, a prototype $\vec{p}_i$ is defined for each class C_i of all the N_i feature vectors $\vec{f}_j$. Each prototype summarizes a painting class, being its *centroid*, calculated in the projected space as:

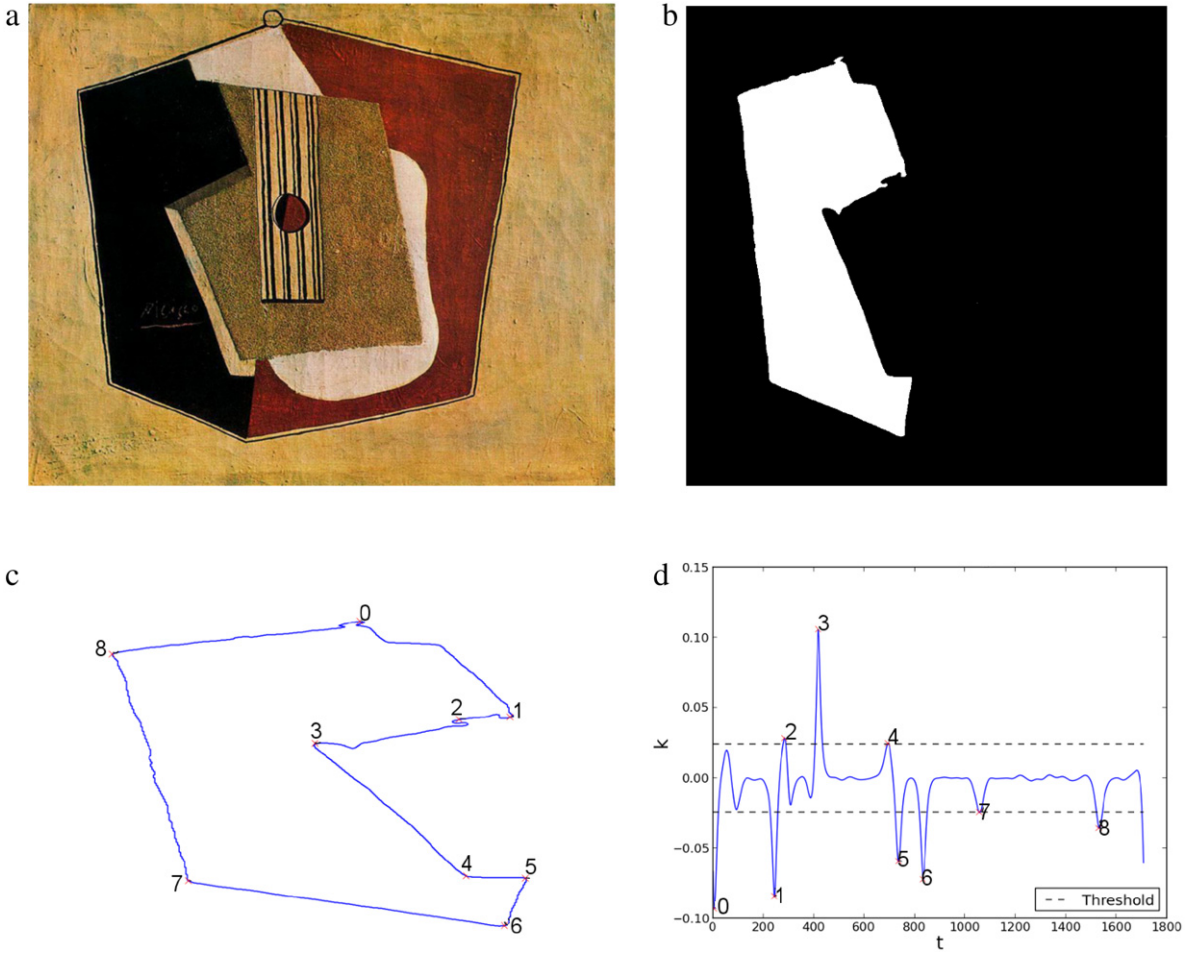$$\vec{p}_i = \frac{1}{N_i}\sum_{j=1}^{N_i}\vec{f}_j. \tag{16}$$

Fig. 2. (a) The original paintings image. (b) A segmented region. (c) The extracted curvature of segment. (d) The parametric curve $k(t)$ with peaks given by a particular threshold.

A sequence S of $\vec{p}_i$ states ordered chronologically defines a time-series. The average state at time i of states $\vec{p}_1$ through $\vec{p}_i$ is defined as:

$$\vec{a}_i = \frac{1}{i} \sum_{j=1}^{i} \vec{p}_j. \tag{17}$$

The opposite state defines an opposition measure from $\vec{p}_i$ as

$$\vec{r}_i = \vec{p}_i + 2(\vec{a}_i - \vec{p}_i) \tag{18}$$

and in this way an opposition vector can be defined:

$$\vec{D}_i = \vec{r}_i - \vec{p}_i. \tag{19}$$

Knowing that any displacement from one state $\vec{p}_i$ to another state $\vec{p}_j$ is defined as

$$\vec{M}_{i,j} = \vec{p}_j - \vec{p}_i \tag{20}$$

it is possible to define an *opposition index* to quantify how much a prototype $\vec{p}_j$ opposes $\vec{p}_i$ (a displacement in direction of $\vec{r}_i$) or emphasizes $\vec{p}_i$ (a displacement in $-\vec{r}_i$ direction):

$$W_{i,j} = \frac{\left\langle \vec{M}_{i,j}, \vec{D}_i \right\rangle}{\|\vec{D}_i\|^2}. \tag{21}$$

However, the movements in such *painting space* are not restricted to confirmation or refutation of "ideas". Alternative ideas can exist out of this dualistic displacement. When an idea shows an alternative movement – besides the opposition

Table 3
Extracted features.

Number of features	Features
4	Energy μ of image rows
4	Energy σ of image rows
4	Energy μ of image columns
4	Energy σ of image rows
4	Energy centroids of image rows
4	Energy centroids of image columns
4	Energy μ of rows and columns
4	Energy σ of rows and columns
4	Angular second moment
4	Contrast
4	Correlation
4	Sum of squares: variance
4	Inverse difference moment
4	Sum average
4	Sum variance
4	Sum entropy
4	Entropy
4	Difference average
4	Difference entropy
4	Correlation coeff. 1
4	Correlation coeff. 2
4	Max. correlation coeff.
2	μ of distance between curvature peaks
2	σ of distance between curvature peaks
1	μ of number of curvature peaks
1	μ of segments perimeter
1	μ of segments area
1	μ of circularity (Per.^{2}/Area)
1	μ of number of segments
1	μ of convex-hull area
1	μ of convex-hull and original areas ratio
99	Total of extracted features

movement – that explores a new region of the *painting space*, it is said the idea is an innovation. This is modeled as a *skewness index* which quantifies how much a prototype $\vec{p}_j$ is innovative when compared with $\vec{p}_i$:

$$s_{i,j} = \sqrt{\frac{|\vec{p}_i - \vec{p}_j|^2 |\vec{a}_i - \vec{p}_i|^2 - [(\vec{p}_i - \vec{p}_j)(\vec{a}_i - \vec{p}_i)]^2}{|\vec{a}_i - \vec{p}_i|^2}}. \tag{22}$$

Another measure arises when considering three consecutive states at times i, j and k. $\vec{p}_i$ being the thesis, $\vec{p}_j$ the antithesis and $\vec{p}_k$ the synthesis, a *counter-dialectics index* can be defined as being

$$d_{i \rightarrow k} = \frac{\left| \langle \vec{p}_j - \vec{p}_i, \vec{p}_k \rangle + \frac{1}{2} \langle \vec{p}_i - \vec{p}_j, \vec{p}_i + \vec{p}_j \rangle \right|}{|\vec{p}_j - \vec{p}_i|} \tag{23}$$

or, the distance between $\vec{p}_k$ and the perpendicular bisector (or middle-hyperplane for N_f-dimensional spaces) between $\vec{p}_i$ and $\vec{p}_j$. In other words, a $\vec{p}_k$ state with higher $d_{i \rightarrow k}$ is far from the synthesis (low dialectics) and vice-versa.

2.5. Feature selection

To select the most relevant features a dispersion measure of the clusters is applied using scatter matrices [15]. For all the N_p paintings, considering all possible combinations of feature pairs $F_{N_p,a}$ and $F_{N_p,b}$, the S_b (between class) and S_w (within class) scatter matrices are calculated with $K = 12$ classes, one class C_i for each painter:

$$S_w = \sum_{i=1}^{K} S_i \tag{24}$$

$$S_b = \sum_{i=1}^{K} N_i (\vec{\mu}_i - \vec{M})(\vec{\mu}_i - \vec{M})^T \tag{25}$$

with N_i the number of paintings in class C_i and the scatter matrix for class C_i defined as

$$S_i = \sum_{i \in C_i} (\vec{f}_i - \vec{\mu}_i)(\vec{f}_i - \vec{\mu}_i)^T \tag{26}$$

Table 4
Feature pairs $F_{N_p,a}$ and $F_{N_p,b}$ ordered by α. Pairs with higher α present better dispersion and clustering. The best feature pairs μ *of curvature peaks* and μ *of number of segments* are selected for analysis and metrics calculation.

Pair nr.	Feature a	Feature b	α
1	μ of curvature peaks	μ of number of seg.	42.445
2	μ of number of seg.	μ of convex-hull area	37.406
3	μ of segments perimeter	μ of number of seg.	36.703
4	μ of segments area	μ of number of seg.	36.214
5	μ of number of segments	μ convex/original	34.885
6	μ of circularity (Per.^{2}/Area)	μ of number of seg.	33.540
7	Energy μ of image rows (green)	μ of number of seg.	32.954
8	Energy μ of rows and columns (green)	μ of number of seg.	32.954
9	Energy σ of image rows (green)	μ of number of seg.	32.932
10	Energy σ of rows and columns (green)	μ of number of seg.	32.906
11	μ of local entropy (5-size window)	μ of number of seg.	32.898
12	Entropy (Haralick adj. 4)	μ of number of seg.	32.898
13	Entropy (Haralick adj. 3)	μ of number of seg.	32.883
14	Entropy (Haralick adj. 1)	μ of number of seg.	32.874
15	Entropy (Haralick adj. 2)	μ of number of seg.	32.869
16	Energy μ of image rows ($r.$)	μ of number of seg.	32.865

where $\vec{f}_i$ is an object of the feature matrix F whose rows and columns correspond to the paintings and its features $F = \left[\leftarrow f_i^T \rightarrow \right]$ and $\vec{\mu}_i$ and $\vec{M}$ are the mean feature vectors for the N_i objects in class C_i and for all the N_p paintings in the projection, respectively:

$$\vec{\mu}_i = \frac{1}{N_i} \sum_{i \in C_i} \vec{f}_i \tag{27}$$

$$\vec{M} = \frac{1}{N_p} \sum_{i=1}^{N_p} \vec{f}_i. \tag{28}$$

The trace of within- and between-class ratio can be used to quantify dispersion:

$$\alpha = \mathrm{tr}(S_b S_w^{-1}). \tag{29}$$

Large values of α reveal larger dispersion and the features which relate with large values of α are selected for the analysis (Section 3.1).

3. Results and discussion

3.1. Best features

By calculating α using Eq. (29) for all possible feature pairs $F_{N_p,a}$ and $F_{N_p,b}$ of the $N_f = 99$ features and ordering the results by α, it is possible to select the features which are most relevant to classification: pairs with high α present better dispersion and clustering than pairs with lower values. As shown in Table 4 (and Fig. 3), features μ *of curvature peaks* and μ *of number of segments* have the higher α and are selected to opposition, skewness and dialectics analysis—both features are shown as predominant also in LDA, discussed in the next section. It is interesting to note the nature of selected features: the number of segments and curvature peaks is the most prominent characteristics for the classification of paintings, even better than texture or image complexity. Other features presenting large values of α – like μ of convex-hull area, segments perimeter and area, and circularity – are also related with shape characteristics. Both features presented a similar projection and clustering properties of Fig. 3 as shown in Fig. A.1.

The projected *painting space* considering all the $K = 12$ groups of paintings that are "represented" by their prototype (i.e. centroid) $\vec{p}_i$ is presented in Fig. 3. The time-series S – a sequence of all the prototype states $\vec{p}_i$ arranged in a chronological order (Section 2.4) – is also shown in the figure as vectors. The projection reveals well clustered groups with minor superposition, mainly for modern paintings.

A striking result is the high distance which Pollock stays when compared with the other painters: it is a consequence of the lag number of segments present in works of Pollock (the y-axis being the projection of this feature: μ *of segments number*). Therefore, both the x-axis (μ *of curvature peaks*) and y-axis are relevant to separate the baroque and modern art movements. It is possible to note a separation between baroque and modern painters where the baroque paintings are arranged in an overlapping group while the modern painters are more clustered and separated from each other while covering a widely region of the *painting space*. This is confirmed by the history of art with modern painters being more individualistic in their styles while baroque painters share aesthetic characteristics in their paintings. The same observation arises when following the time-series, the difference between the movements is clear: while baroque artists tend to present a recurring pattern,
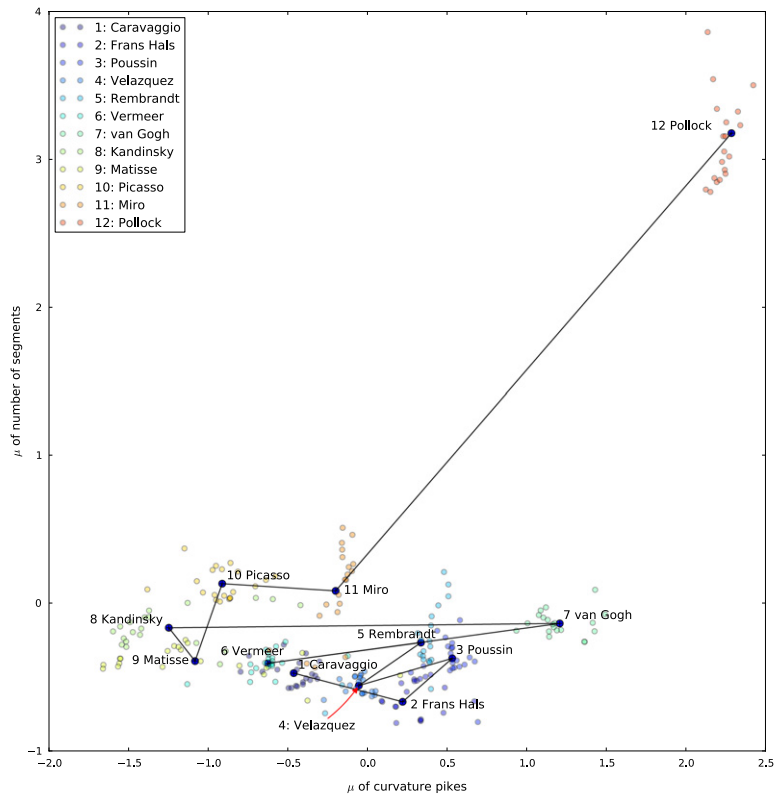
Fig. 3. Projected *painting space* considering the best pair of features: μ *of curvature peaks* and μ *of number of segments*.

an abrupt displacement separates van Gogh – the first modern painter in the *painting space* – from the previous, and breaks the cyclic pattern. van Gogh, although located near the baroque painters and in the opposite extreme of modern painters, represents a transition to the modern period and after him the following vector displacements will continue until the higher transition in Pollock.

Using an index for clustering evaluation – based on Davies–Bouldin [16] index – it is possible to check how clustered each group of paintings is around a given centroid $\vec{p}_i$. This measure is defined as a cluster scattering index T_i for each cluster C_i:

$$T_i = \sqrt{\frac{1}{N_i} \sum_{j=1}^{N_i} |\vec{f}_j - \vec{p}_i|^2}$$

(30)

which represents the mean distance from each painting $\vec{f}_j$ to its centroid $\vec{p}_i$. This index was normalized by a global scattering index $T_{\vec{g}}$:

$$T_{\vec{g}} = \sqrt{\frac{1}{N_p} \sum_{i=1}^{N_p} |\vec{f}_i - \vec{g}|^2}$$

(31)

where $\vec{g}$ is the global centroid: the mean vector considering all N_p paintings. The ratio $T_i/T_{\vec{g}}$ (Table 5) gives a measurement of how scattered each cluster is relative to the global dispersion of paintings. In other words, it is possible to check the uniformity of painting style for a single author: painters with higher $T_i/T_{\vec{g}}$ values present less uniformity of style, while lower values reveal more homogeneous works by a given painter. In general, baroque painters present more homogeneous works than modern painters. Modern painters seem to explore more the *painting space* than baroque painters.

While analyzing the baroque group separately, it is possible to observe a trajectory drawn by Caravaggio and Frans Hals through Poussin which ends with the opposite (and back forth) movement of Velázquez. It can be attributed to the influence of the "*chiaroscuro*" master on these painters, mainly in Velázquez who is known to have studied the works of Caravaggio [12]. It arises again in the return to the Caravaggio movement by Vermeer—some critics affirm [17] that painters like Vermeer could not have even existed without Caravaggio's influence: Vermeer and Caravaggio clusters are the most superimposed considering all the portraits in the *painting space*. Both facts are confirmed by the histograms of gray levels shown in Fig. 4. Velázquez and Vermeer histograms are more similar to Caravaggio's histogram than the remaining baroque painters.

Table 5
Cluster scattering index T_i for each cluster C_i and the ratio between T_i and the global cluster scattering index $T_{\vec{g}}$. The ratio measures how scattered the paintings in a given cluster are. Painters with lower $T_i/T_{\vec{g}}$ values present more homogeneous works than painters with higher values of $T_i/T_{\vec{g}}$.

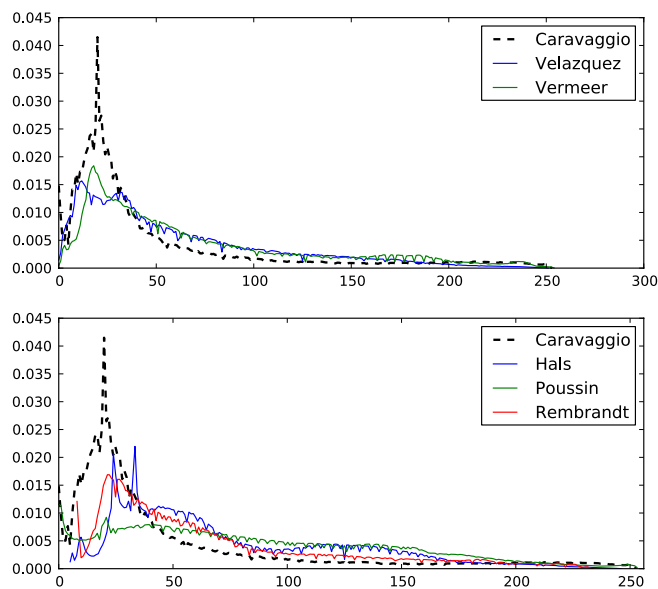| Artists	T_i	$T_i/T_{\vec{g}}$
Caravaggio	0.026	0.110
Frans Hals	0.074	0.302
Poussin	0.028	0.117
Velázquez	0.016	0.066
Rembrandt	0.051	0.212
Vermeer	0.031	0.130
van Gogh	0.029	0.120
Kandinsky	0.063	0.260
Matisse	0.085	0.349
Picasso	0.033	0.139
Miró	0.053	0.217
Pollock	0.073	0.302

Fig. 4. Mean gray levels histograms for all the baroque painters. Vermeer and Velázquez show more similarity with Caravaggio than other baroque painters.

In summary, the baroque group shows a strong inter-relationship by comparing with modern painters where the absence of super-impositions is remarkable. Again, this suggests a strong style-centric distinction among artists of the modern era while baroque artists shared techniques and aesthetic characteristics. This is also confirmed when comparing the histograms of modern paintings in Fig. 5: smaller similarities are observed between the considered artists, contrasting with baroque painters shown in Fig. 4.

When considering opposition and skewness, more interesting results arise, as shown in Table 6 and Fig. 6. Clearly, the larger value for opposition is attributed to Rembrandt. This is surprising given that the Dutch master figures as a "counterpoint" of baroque even being part of this art movement [12]. Vermeer also presents strong opposition and the nature of his paintings (e.g. domestic interior, use of bright colors) could explain this phenomenon. A pattern is shown in the beginning of baroque and modern art: an opposition decrease is present in both cases, which is followed by an increase in opposition. Henceforth, a following plateau of high opposition values is observed in baroque painters. This plateau happens in the transition period between baroque and modern art, gradually decreasing while the modern artists begin to take their place in history. These decreasing opposition values reflect a low opposition role between first artists of baroque period and increasing opposition as long as the period is moving into modernism, although skewness values remain oscillating and increasing during almost all the time-series. This characterizes again a common scene in arts, mostly in modernists, each one trying to define his own style and preparing to change into a new movement. In summary, the *painting space* is marked by constantly increasing skewness, strong opposition in specific moments of its evolution (the transition between baroque and modern) and minor opposition between the artists of the same movement.
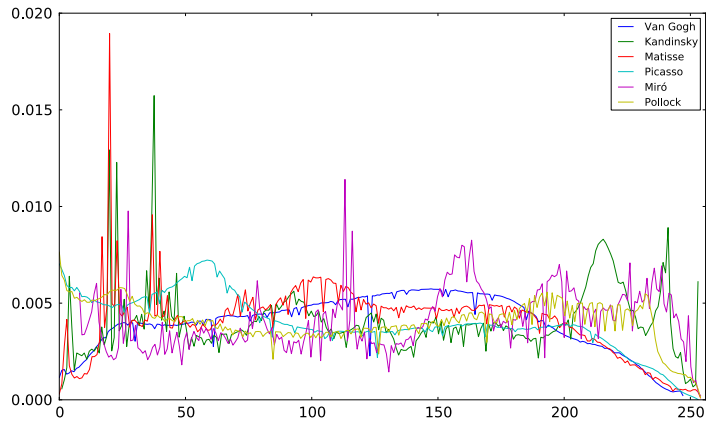
Fig. 5. Mean gray levels histogram for all the modern painters. There are minor similarities between modern artists.
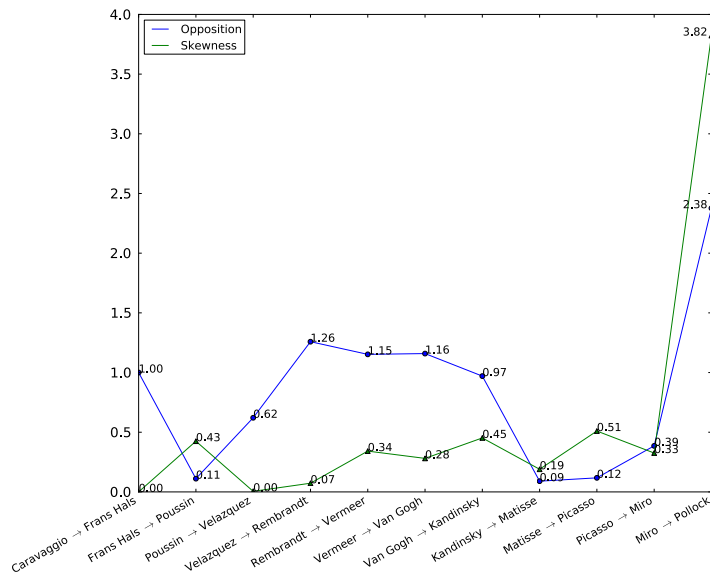

Fig. 6. Opposition $W_{i,j}$ and skewness $s_{i,j}$ values for the two best features.

Table 6
Opposition and skewness indices for each of the twelve moves from a painter to the next.

Painting move	$W_{i,j}$	$s_{i,j}$
Caravaggio → Frans Hals	1.0	0.0
Frans Hals → Poussin	0.111	0.425
Poussin → Velázquez	0.621	0.004
Velázquez → Rembrandt	1.258	0.072
Rembrandt → Vermeer	1.152	0.341
Vermeer → van Gogh	1.158	0.280
van Gogh → Kandinsky	0.970	0.452
Kandinsky → Matisse	0.089	0.189
Matisse → Picasso	0.117	0.509
Picasso → Miró	0.385	0.325
Miró → Pollock	2.376	3.823

The counter-dialectics, shown in Table 7 and Fig. 7, draws a parallel with the opposition and skewness curves. It reinforces the already observed facts: painters of the same movement show initially decreasing followed by increasing counter-dialectics reflecting the concordance of members of the same movement and their preparation to change into the next movement. The larger counter-dialectics happens in van Gogh and Kandinsky: again, the point where baroque ends and modern art starts, regarding the painters selected for this study.
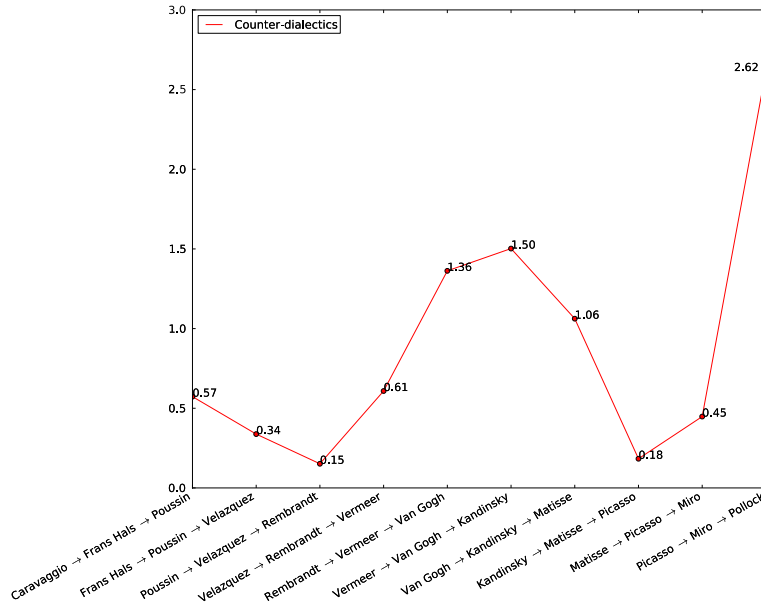
Fig. 7. Counter-dialectics values considering the two best features.

Table 7
Counter-dialectics index for each of the ten subsequent moves among painters states for the best two features.

Painting triple	$d_{i \to k}$
Caravaggio → Frans Hals → Poussin	0.572
Frans Hals → Poussin → Velázquez	0.337
Poussin → Velázquez → Rembrandt	0.151
Velázquez → Rembrandt → Vermeer	0.608
Rembrandt → Vermeer → van Gogh	1.362
Vermeer → van Gogh → Kandinsky	1.502
van Gogh → Kandinsky → Matisse	1.062
Kandinsky → Matisse → Picasso	0.183
Matisse → Picasso → Miró	0.447
Picasso → Miró → Pollock	2.616

Table 8
Opposition and skewness indices for each of the twelve painters states moves.

Painting move	$W_{i,j}$	$s_{i,j}$
Caravaggio → Frans Hals	1.0	0.0
Frans Hals → Poussin	−0.101	0.132
Poussin → Velázquez	0.588	0.037
Velázquez → Rembrandt	1.526	0.050
Rembrandt → Vermeer	1.101	0.143
Vermeer → van Gogh	1.153	0.157
van Gogh → Kandinsky	1.279	0.512
Kandinsky → Matisse	0.179	0.149
Matisse → Picasso	−0.201	0.516
Picasso → Miró	0.432	0.163
Miró → Pollock	4.031	2.662

3.2. All the features

Although features $F_{N_p,a}$ (μ of curvature peaks) and $F_{N_p,b}$ (μ of number of segments) are shown as an interesting choice for classification, LDA is applied considering all the $N_f = 99$ features to test the relevance of these features and the stability of the results. The LDA method [15] projected the features in a 2-dimensional space that better separates the paintings and yields a time-series as done for the two most prominent features. The first two components give the time-series shown in Fig. 8. It is possible to note, as expected, a similarity with results from Section 3.1. The skewness indices show even more an ascending curve along the entire evolution, as presented in Table 8 and Fig. 9. The opposition and dialectics (Table 9 and Fig. 10) patterns remain.
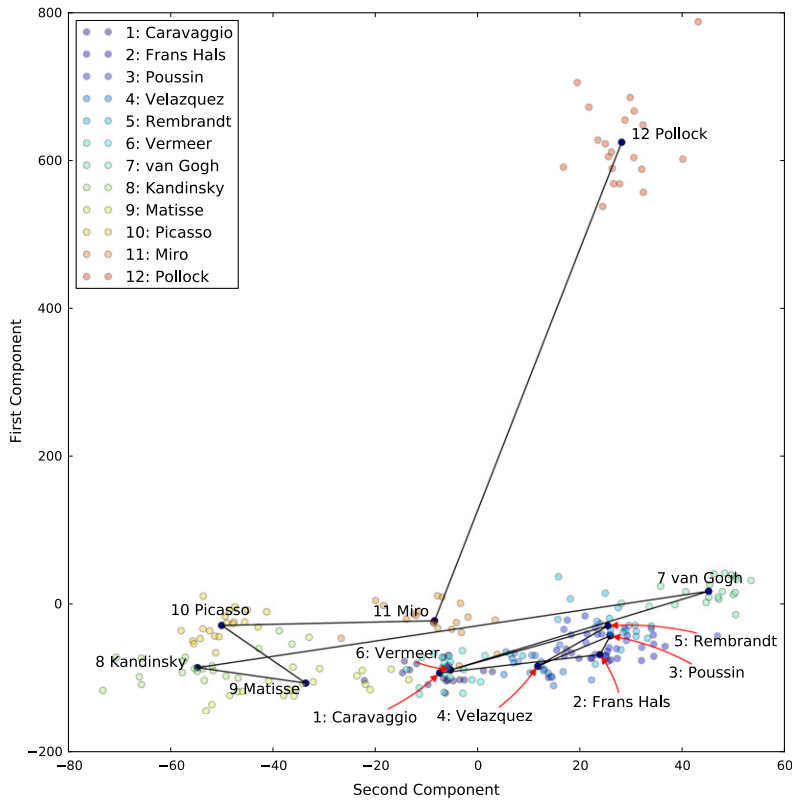
Fig. 8. Time series yielded by 2-dimensional projected "painting space" considering the two first components obtained by LDA transformed into the $N = 99$ feature matrix.
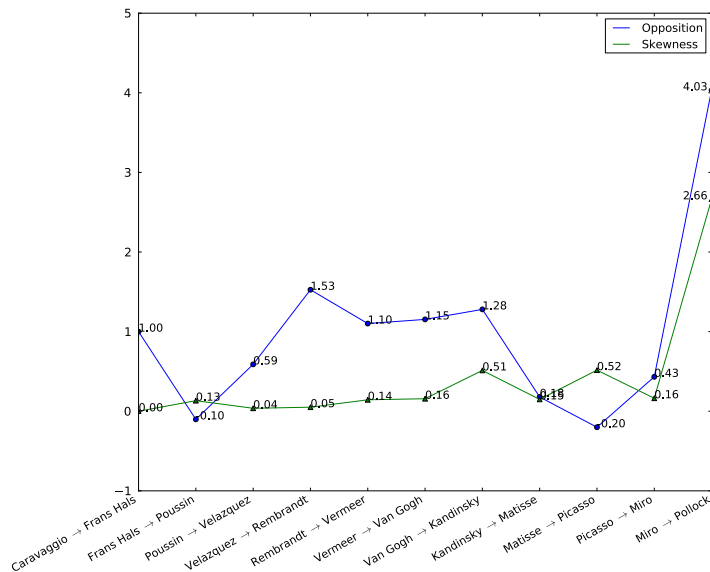

Fig. 9. Opposition and Skewness values considering the time series for all the features. The same patterns observed when analyzing the best feature pair remains in this observation.

For LDA validation, the total set of paintings is split into two groups: a training set with 10 random selected paintings for each artist and a test set with the remaining 10 paintings for each artist, without repetition. Such a validation is performed 100 times. The confusion matrix (Fig. 11) reveals the quality of the predicted output. Diagonal elements represent the mean number of samples for which the predicted class is equal to the true class, while off-diagonal elements indicate the ones that are unclassified by LDA. Higher diagonal values indicate more correct predictions. As observed, the LDA method performed

Table 9
Counter-dialectics index for each of the ten subsequent moves among painters states for the best two components of LDA projection.

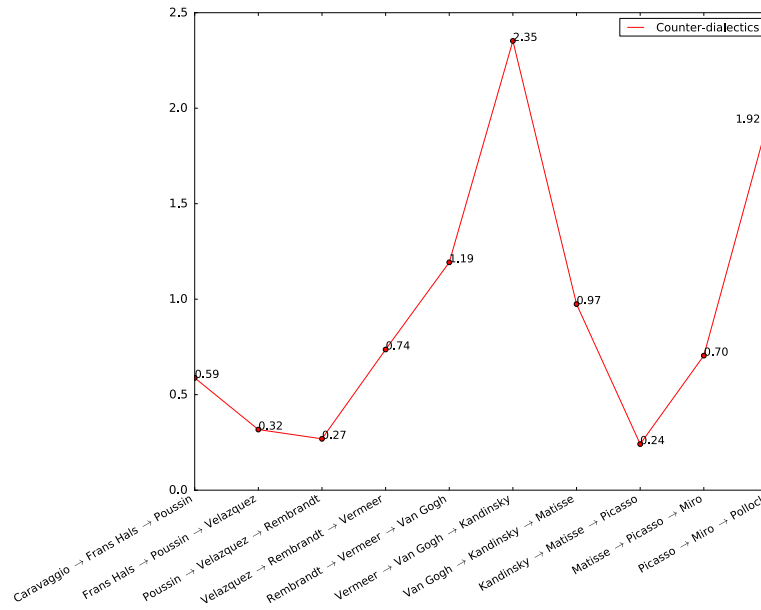| Painting triple	$d_{i \to k}$
Caravaggio → Frans Hals → Poussin	0.587
Frans Hals → Poussin → Velázquez	0.317
Poussin → Velázquez → Rembrandt	0.268
Velázquez → Rembrandt → Vermeer	0.736
Rembrandt → Vermeer → van Gogh	1.192
Vermeer → van Gogh → Kandinsky	2.352
van Gogh → Kandinsky → Matisse	0.974
Kandinsky → Matisse → Picasso	0.241
Matisse → Picasso → Miró	0.704
Picasso → Miró → Pollock	1.924

Fig. 10. Counter-dialectics values (higher values reveal lower dialectics) considering all the features. The pattern observed in the best pair projection became stronger here: it is possible to observe clearly the highest value along the movement transition period (van Gogh and Kandinsky).

as expected for the considered set of paintings. The best classified samples are Pollock paintings which is expected given the high detachment of this cluster observed in the presented projections. In general, the confusion matrix reflects facts previously discussed: a similarity between baroque painters, mainly Velázquez, Caravaggio and Rembrandt and a separation between painters before and after van Gogh which defines the frontier between the baroque and modern movements.

4. Conclusions

It is shown that two features: (a) the number of curvature peaks and (b) the number of segments of an image – both related with shape characteristics – can be used for the classification of the selected painters with remarkable results, even when compared with canonical feature measures like Haralick or image complexity. Such relevance is supported by the analysis of a dispersion index calculated for every pair of features and reinforced by LDA analysis.

The effective characterization of selected paintings by means of these features allowed the definition of a "*painting space*". While represented as states in this projected space, the baroque paintings are shown as an overlapped cluster. The modern paintings clusters, in contrast, present minor overlapping and are disposed more widely in the projection. These observations are compatible with the history of art: baroque painters shared aesthetics while modern painters tend to define their own styles individually [12].

A time-series – composed by prototype states representing each painter chronologically – allowed the concepts of opposition, skewness and dialectics to be approached quantitatively, as geometric measures. The painting states show a decrease in opposition and dialectics considering the first members of the same movement (baroque or modern) followed by increasing opposition and dialectics until it reaches the strong opposition momentum between the two movements. Also, the skewness curve increases during almost entire time-series. This could reflect a strong influence role of a movement in its members together with an increasing desire to innovate, present in each artist, stronger in modernists.
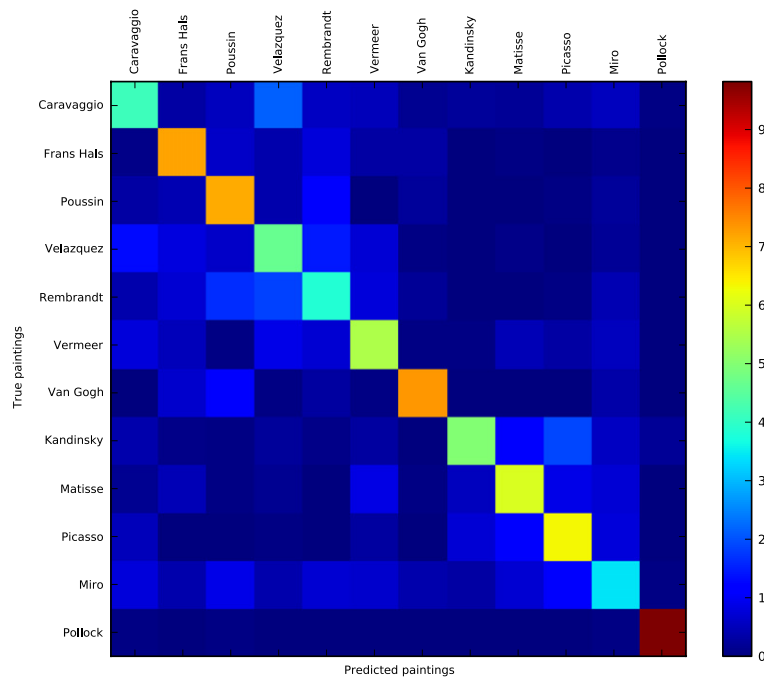
Fig. 11. Confusion matrix for LDA. Half of the paintings are used as a training set and the other half as a test set. The validation is performed 100 times. Diagonal elements show the mean number of paintings in the predicted class (a painter) which equals the true class.

Both opposition, skewness and dialectics measurements can be compared with results already obtained for music and philosophy [11]. Music composers seem to be guided by strong dialectics due to the recognized master–apprentice role. Philosophers movements, otherwise, are strong in opposition. Painters, as this study reveals, show increasing skewness, and strong values for both opposition and counter-dialectics in specific moments of history—i.e. baroque–modern transition.

While not sufficient to exhaust all the characteristics regarding an artist or its work, this method suggests a framework to the study of arts by means of a feature space and geometrical measures. As a future work, the number of painters could be increased and a set of painters could be specifically chosen to analyze influence (e.g. works of Frans Hals' sons can be included to verify the influence of their father and master, or paintings by Rafael, Poussin and Guido Reni [12] or Carracci can be compared to confront the already known similarity of both painters). A larger number of paintings for each artist could be considered for analysis as well. Although this study promotes a quantitative approach, qualitative features can be used, as done in a previous work for musicians and philosophers [11]. A comparison between results obtained for quantitative and qualitative features can then be applied. The same framework can be applied to other fields of interest like Movies or Poetry. Another interesting use of this framework – being currently developed by the authors – is a component of a generative art model: geometrical measures in the *painting space* (like the already defined dialectics or opposition and skewness) can guide an evolutionary algorithm, assigning the value of measures as the fitness of generated material. This model complements a framework to the study of creative evolution in arts.

Acknowledgments

Appendix A

Although the first features pair (μ of curvature peaks and μ of number of segments) is selected for the analysis, other features with large α values can be used as shown in Fig. A.1.

Appendix B

See Table B.1.
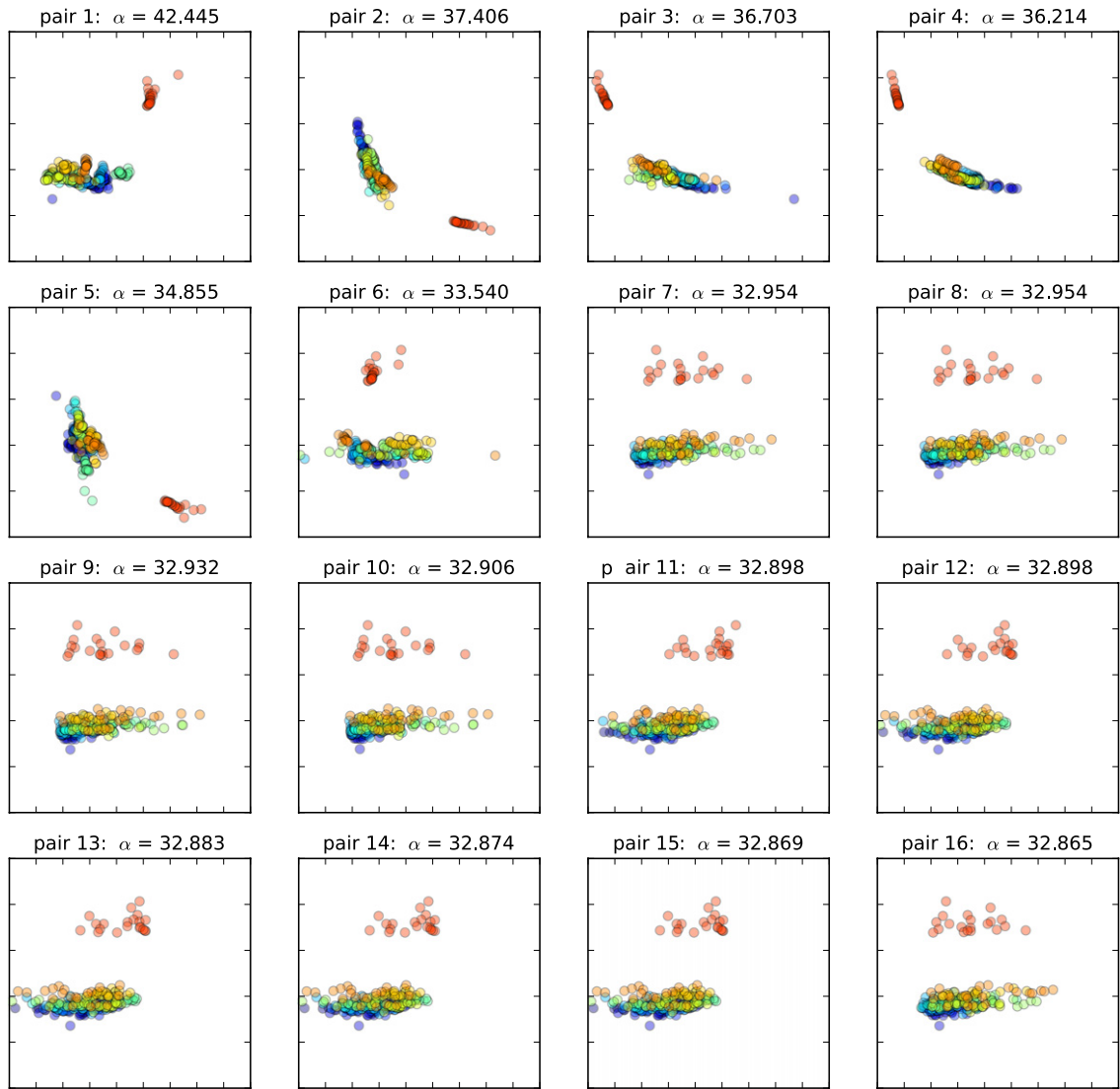
Fig. A.1. Scatter plots for each feature pair *i* listed in Table 4 with large values of α. The first projection (pair 1) was used for the analysis, however other projections (pairs 2–16) can be used.

Table B.1
All the 240 selected paintings and their respective authors and years of creation.

Painter	Painting title	Year
Caravaggio	Musicians	1595
	Judith Beheading Holofernes	1598
	David with the Head of Goliath	1610
	Supper at Emmaus	1602
	Entombment	1603
	Narcissus	1599
	John the Baptist	1610
	Denial of Saint Peter	1610
	Tooth Puller	1609
	Annunciation	1608
	Sleeping Cupid	1608
	Beheading of Saint John the Baptist	1608
	Saint Jerome Writing	1607
	Salome with the Head of John the Baptist	1607
	Christ at the Column	1607

(*continued on next page*)

Table B.1 (*continued*)

Painter	Painting title	Year
	Madonna and Child with St. Anne	1606
	Ecce Homo	1605
	John the Baptist	1604
	Madonna of Loreto	1604
	Taking of Christ	1602
Frans Hals	Portrait of an unknown woman	1618/20
	Portrait of Paulus van Beresteyn	1620s
	Portrait of Stephanus Geeraerdts	1648/50
	Portrait of Pieter van der Broecke	1633
	Portrait of a man	1645
	Portrait of Ren Descartes	1649
	Regenten of the Grote of St. Elisabeth Gasthuis	1641
	Portrait of Isaak Abrahamsz Massa	1626
	The Officers of the St Adrian Militia Company	1633
	Two singing boys with a lute and a music book	1620/25
	The rommelpot player	1618/22
	The 'Mulatto'	1628/30
	Wedding portrait of Isaac and Beatrix	1622
	The Banquet of the Officers of the St George Militia	1627
	Portrait of the family Gijsbert Claesz van Campen	1620
	Young Man and Woman in an Inn	1623
	Shrovetide Revellers	1616/17
	Laughing man with crock	1628/30
	Young Man with a Skull	1626/28
	Young woman (The Gypsy Girl—Malle Babbe)	1625
Nicolas Poussin	Venus and Adonis	1624
	Cephalus and Aurora	1627
	Acis and Galatea	1629
	The Adoration of the Golden Calf	1634
	A Dance to the Music of Time	1633
	Apollo and Daphne or Apollo in love with Daphne	1664
	The Four Seasons: Autumn	1660/64
	The Four Seasons: Spring	1660/64
	Landscape with Hercules and Cacus	1659/61
	Queen Zenobia found on the banks of the river Arax	1657/60
	Lamentation over the dead Christ	1657/58
	The Flight into Egypt or resting on the journey	1657/58
	Saint John baptizing Christ	1648
	The Miracle of saint Francis Xavier	1641/42
	The Institution of the Eucharist	1641
	Landscape with saint John on Patmos	1640
	Venus presenting arms to Aeneas	1639
	Finding of Moses	1638
	Camillus hands over the schoolmaster of Falerii	1637
	The Triumph of Neptune or The Birth of Venus	1635
Diego Velázquez	Three musicians	1617/18
	The Lunch	1618
	La mulata	1620
	Old Woman Cooking Eggs	1618
	Christ in the House of Martha and Mary	1618
	Adoration of the Magi	1619
	Demócrito/El geógrafo	1628/29
	The Triumph of Bacchus	1628/29
	La cena de Emaús	1628/29
	Joseph's Tunic	1630
	Temptation of St. Thomas	1631/32
	Las Meninas	1656/57
	Christ Crucified	1632
	Equestrian Portrait of the Count-Duke of Olivares	1634
	The Surrender of Breda	1634/35
	The Needlewoman	1635/43
	The Jester Calabacillas	1637/39
	Menipo	1639/41
	Mars Resting	1639/41
	Rokeby Venus	
Rembrandt	The Spectacles-pedlar (Sight)	1624/25
	The Three Singers (Hearing)	1624/25
	Balaam and the Ass	1626

Table B.1 (*continued*)

Painter	Painting title	Year
	History Painting	1626
	The Baptism of the Eunuch	1626
	Andromeda	1630
	St. Peter in Prison	1631
	The Anatomy Lesson of Dr. Tulp	1632
	The Rape of Europa	1632
	Christ in the Storm on the Sea of Galilee	1633
	Diana Bathing with her Nymphs	1634
	The Company of Captain Frans Banning Cocq	1642
	The Holy Family with Angels	1645
	Bathsheba Bathing	1645
	A Woman Bathing in a Stream	1654
	The Syndics of the Draper's Guild	1662
	Self-portrait	1660
	The Polish Rider	1657
	The Anatomy Lesson of Dr. Jan Deyman	1656
	Jacob Blessing the Children of Joseph	1656
Johannes Vermeer	Lady Seated at a Virginal	1673/75
	The Guitar Player	1672
	Lady Writing a Letter with her Maid	1670
	The Love Letter	1669/70
	The Lacemaker	1669/70
	The Geographer	1668/69
	The Astronomer	1668
	Girl with a Red Hat	1668
	Mistress and Maid	1667/68
	The Allegory of Painting	1666/67
	Portrait of a Young Woman	1666/67
	Girl with a Pearl Earring	1665
	Girl Interrupted at her Music	1660/61
	The Girl with the Wineglass	1659
	The Milkmaid	1658
	Christ in the House of Martha and Mary	1654/55
	Diana and Her Companions	1655/56
	Girl Reading a Letter at an Open Window	1657
	A Girl Asleep	1657
	The Music Lesson	1662/65
Vincent van Gogh	Starry Night Over the Rhone	1888
	The Starry Night	1889
	Self-Portrait with Straw Hat	1887/88
	A Wheat Field, with Cypresses	1889
	Wheat Field with Crows	1890
	The Red Vineyard	1888
	Still Life: Vase with Fifteen Sunflowers	1889
	Self-Portrait with Bandaged Ear	1889
	Prisoners' Round	1890
	Road with Cypress and Star	1890
	Bedroom in Arles	1889
	Child with Orange	1890
	Portrait of Dr. Gachet	1890
	Cypresses and Two Women	1890
	The Sower with Setting Sun	1888
	Olive Grove: Orange Sky	1889
	Mountains at Saint-Rémy	1889
	Olive Orchard	1889
	Olive Trees in a Mountainous Landscape	1889
	View of the Asylum and Chapel of Saint-Rémy	1889
Wassily Kandinsky	On White II	1923
	Composition X	1939
	Points	1920
	Ensemble Multicolore	1938
	Composition VIII	1923
	Composition VI	1913
	Composition IV	1911
	Farbstudie Quadrate	1913
	Black and Violet	1923
	Yellow, Red, Blue	1925

Table B.1 (*continued*)

Painter	Painting title	Year
	At Rest	1942
	Conglomerat	1943
	Temperered Elan	1944
	Last Watercolour	1944
	Untitled	1944
	Composition	1944
	White Figure	1943
	A Floating Figure	1942
	Intime Message	1942
	Reciprocal Accords	1942
Henri Matisse	Self-Portrait in a Striped T-shirt	1906
	Portrait of Madame Matisse	1905
	Le bonheur de vivre	1905/6
	The Dance (first version)	1909
	Blue Nude	1907
	Portrait of the Artist's Wife	1913
	The Moroccans	1915/16
	The Gourds	1916
	Bathers by a River	1909/16
	La Nu Rose	1935
	Reclining Nude	1917
	Dancer and Rocaille Armchair on a Black Background	1942
	Asia	1946
	Red Interior, Still Life on Blue Table	1947
	Still Life	
	Still Life 14	
	Head white and pink	
	Woman In A Purple Coat	1937
	Still Life after Jan Davidsz. de Heem's "La Desserte"	1915
	Coffee	1917
Pablo Picasso	Les Demoiselles d'Avignon	1907
	Guernica	1937
	Dora Maar au Chat	1941
	Massacre in Korea	1951
	The Guitar	
	Arlequín	1917
	La Table	1919
	Woman with Pears	1909
	Femme nue assise	1909
	Le pigeon aux petits pois	1911
	Guitar, Bottle, Fruit Dish and Glass on a Table	1919
	Lovers	1919
	Jacqueline	1961
	Femme au chapeau assise dans un fauteuil (Dora Maar)	1941
	Seated woman	1953
	Jacqueline with flowers	1954
	Les femmes d'Alger	1954
	Les femmes d'Alger XV	1955
	Deux Femmes Sur La Plage	1956
	Portrait of woman (Dora Maar)	1942
Joan Miró	The Farm	1921/22
	The Tilled Field	1923/24
	Bleu II	1961
	Nocturne	1940
	Le Coq	1940
	Figure at Night Guided by (…)	1940
	Dancer	1925
	Harlequin's Carnival	1924/25
	Person Throwing a Stone at a Bird	1926
	Painting	1936
	Woman Encircled by the Flight (…)	1941
	The Bull Fight	1945
	The Smile of the Flamboyant Wings	1953
	Hermitage	1924
	Maternity	1924
	Landscape	1924/25
	Head of a Catalan Peasant (2)	1925

Table B.1 (*continued*)

Painter	Painting title	Year
	Nude	1926
	The Hunter	1923/24
	Ciphers and Constellations, in Love with a Woman	1941
Jackson Pollock	No. 5	1948
	Black and White (Number 20)	1951
	Number 8	1949
	Number 11	1952
	Number 31	1950
	Number 1	1948
	Number 3 (Tiger)	1949
	Untitled	1942
	Alchemy	1947
	Number 23	1948
	Galaxy	1947
	Enchanted Forest	1947
	Lucifer	1947
	Reflection of the Big Dipper	1947
	Number 4 (Gray and Red)	1948
	Summertime: Number 9A	1948
	Number 6	1949
	Autumn Rhythm	1950
	Blue Poles	1952
	Number 7	1949

References

[1] AnaIoana Deac, Jan Lubbe, Eric Backer, Feature selection for paintings classification by optimal tree pruning, in: Bilge Gunsel, Anil K. Jain, A.Murat Tekalp, Bülent Sankur (Eds.), Multimedia Content Representation, Classification and Security, in: Lecture Notes in Computer Science, vol. 4105, Springer, Berlin, Heidelberg, 2006, pp. 354–361.

[2] Oguz Icoglu, Bilge Gunsel, Sanem Sariel, Classification and indexing of paintings based on art movements, in: Proc. of EUSIPCO, 2004, pp. 749–752.

[3] M. Spehr, C. Wallraven, R.W. Fleming, Image statistics for clustering paintings according to their visual appearance, in: Proceedings of the Fifth Eurographics Conference on Computational Aesthetics in Graphics, Visualization and Imaging, Computational Aesthetics'09, Eurographics Association, Aire-la-Ville, Switzerland, 2009, pp. 57–64.

[4] C.R. Johnson, E. Hendriks, I.J. Berezhnoy, E. Brevdo, S.M. Hughes, I. Daubechies, Jia Li, E. Postma, J.Z. Wang, Image processing for artist identification, IEEE Signal Process. Mag. 25 (4) (2008) 37–48.

[5] Lev Manovich, Style space: how to compare image sets and follow their evolution (Draft text), August 2011. http://lab.softwarestudies.com/2011/08/style-space-how-to-compare-image-sets.html.

[6] Lev Manovich, Mondrian vs Rothko: footprints and evolution in style space, June 2011. http://lab.softwarestudies.com/2011/06/mondrian-vs-rothko-footprints-and.html.

[7] Lev Manovich, Arthistory.viz—visualizing modernism, November 2008. http://lab.softwarestudies.com/2008/07/arthistoryviz-mining-200000-images-of.html.

[8] Juan Romero, Penousal Machado, Adrian Carballal, Antonino Santos, Using complexity estimates in aesthetic image classification, J. Math. Arts 6 (2–3) (2012) 125–136.

[9] J. Zujovic, L. Gandy, S. Friedman, B. Pardo, T.N. Pappas, Classifying paintings by artistic genre: an analysis of features and classifiers, in: IEEE International Workshop on Multimedia Signal Processing, 2009. MMSP'09, 2009. pp. 1–5.

[10] H.L. Williams, Hegel, Heraclitus, and Marx's Dialectic, St. Martin's Press, 1989.

[11] Vilson Vieira, Renato Fabbri, Gonzalo Travieso, Osvaldo N. Oliveira Jr., Luciano da Fontoura Costa, A quantitative approach to evolution of music and philosophy, J. Stat. Mech. Theory Exp. 2012 (08) (2012) P08010.

[12] E.H. Gombrich, The Story of Art, in: Story of Art, Phaidon Press, Ltd., 1995.

[13] Radhakrishna Achanta, Appu Shaji, Kevin Smith, Aurélien Lucchi, Pascal Fua, Sabine Süsstrunk, SLIC superpixels compared to state-of-the-art superpixel methods, IEEE Trans. Pattern Anal. Mach. Intell. 34 (11) (2012) 2274–2282. A previous version of this article was published as a EPFL Technical Report in 2010: http://infoscience.epfl.ch/record/149300. Supplementary material can be found at: http://ivrg.epfl.ch/research/superpixels.

[14] Robert M. Haralick, Karthikeyan Shanmugam, Its' Hak Dinstein, Textural features for image classification, IEEE Trans. Syst. Man Cybern. (6) (1973) 610–621.

[15] Luciano da Fontoura Da Costa, Roberto Marcondes Cesar Jr., Shape Analysis and Classification: Theory and Practice, first ed., CRC Press, Inc., Boca Raton, FL, USA, 2000.

[16] D.L. Davies, D.W. Bouldin, A cluster separation measure, IEEE Trans. Pattern Anal. Mach. Intell. (2) (1979) 224–227.

[17] G. Lambert, G. Néret, Caravaggio. Ediz. tedesca, in: Basic Art Series, Taschen Deutschland GmbH, 2000.